Optics Letters

Tailorable dispersion in a four-wave mixing laser

Demetrious T. Kutzke,[1] Owen Wolfe,[1] Simon M. Rochester,[2] Dmitry Budker,[2,3,4] Irina Novikova,[1] and Eugeniy E. Mikhailov[1,*]

[1]Department of Physics, College of William & Mary, Williamsburg, Virginia 23187, USA
[2]Rochester Scientific, LLC, El Cerrito, California 94530, USA
[3]Department of Physics, University of California, Berkeley, California 94720-7300, USA
[4]Helmholtz Institute Mainz, Johannes Gutenberg University, 55099 Mainz, Germany
*Corresponding author: eemikh@wm.edu

Received 8 May 2017; revised 26 June 2017; accepted 26 June 2017; posted 27 June 2017 (Doc. ID 295620); published 14 July 2017

We present experimental results demonstrating controllable dispersion in a ring laser by monitoring the lasing-frequency response to cavity-length variations. Pumping on an N-type level configuration in ^{87}Rb, we tailor the intra-cavity dispersion slope by varying experimental parameters, such as pump-laser frequency, atomic density, and pump power. As a result, we can tune the pulling factor, i.e., the ratio of the laser frequency shift to the empty cavity frequency shift, of our laser by more than an order of magnitude.

OCIS codes: (270.1670) Coherent optical effects; (270.4180) Multiphoton processes; (270.3430) Laser theory.

https://doi.org/10.1364/OL.42.002846

The sensitivity of a cavity's resonant frequency to changes in its optical path length is at the heart of many interferometric optical measurements [1]. This effect is employed in lasers to tune their operating frequency, and in precision path-length measurements to permit a distance measurement resolution at the sub-atomic-length scale (as required for the detection of gravitational waves [2]). State-of-the-art high-finesse cavities are capable of seeing a frequency shift due to one excited atom in the cavity, providing the basis for cavity-quantum-electrodynamic tests [3]. The same effect, employed in optical gyroscopes, allows detection of minuscule changes in rotation speed [4,5].

All of the above is reflected in the standard textbook formula governing the frequency shift Δf_{empty} of an empty cavity with respect to a change in its round-trip path length p: $\Delta f_{\text{empty}} = -f_0 \frac{\Delta p}{p}$, where f_0 is the resonant frequency for the path length p. However, if there is a medium inside the cavity, then the cavity response must account for the dispersion of the medium [6]:

$$\Delta f_{\text{dispersive}} = \Delta f_{\text{empty}} \frac{1}{n_0 + f_0 \frac{\partial n}{\partial f}} = \Delta f_{\text{empty}} \frac{1}{n_g}, \quad (1)$$

where n_g is the group refractive index, n_0 is the refractive index at the light frequency f_0, and $\frac{\partial n}{\partial f}$ is the dispersion.

If the dispersion is positive and sufficiently large, then $n_g \geq 1$. This suppresses the cavity sensitivity to length perturbations. The regime with $n_g \geq 1$ is called the subluminal or the slow-light regime, since the group velocity $v_g = c/n_g < c$. This regime is useful in producing stable laser systems, where the laser frequency is immune to cavity-length fluctuations [7].

If the dispersion is negative and sufficiently large, then $n_g \leq 1$. This is known as the superluminal or the fast-light regime, since the group velocity exceeds the speed of light in vacuum. In this regime, the cavity response to the path change is enhanced. For the extreme case of $n_g = 0$, Eq. (1) seems to indicate that the resonance frequency has an infinite response to a cavity path-length change; however, an infinite number of round trips is required to achieve the steady state [8]. Nevertheless, a quite significant enhancement of the cavity response can theoretically be achieved, as suggested for cases of passive cavities filled with dispersive media [9,10] and cavities with actively controlled atomic dispersion [6,11]. For the passive-cavity case, there has been experimental demonstration of increasing cavity response by a factor exceeding 300 [12].

So far, there has been no direct demonstration of the *dispersion-modified laser-frequency* dependence on the cavity path change. The goal of this Letter is to directly show the tailorable intra-cavity dispersion of the lasing cavity via its modified response. We demonstrate that the cavity response can be changed by more than an order of magnitude by varying experimental parameters.

Maintaining the fast-light regime for a lasing field is challenging. Due to the Kramers–Kronig relationship, an amplification line has positive dispersion, which is associated with the slow-light regime. To circumvent this, there must be a local absorption dip in the overall laser gain line.

We base our setup on an N-configuration pumping scheme outlined in [13]. In this scheme, two strong pump lasers are tuned in the vicinity of the D_1 and the D_2 Rb lines, as shown in Fig. 1. This creates favorable conditions for four-wave mixing (FWM) of the pumps and the two additional new fields α and β that result from the Raman-gain conditions. The D_1 pump field by itself creates subluminal conditions for the α field. In the presence of the strong D_2 pump, however, the gain line of the α field splits, which creates the dip necessary for the fast-light regime. The D_2 pump also increases the gain for α via the FWM process. During our preliminary studies on the

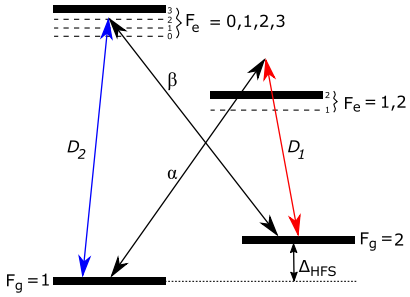

Fig. 1. Four-wave mixing pumping N-scheme and relevant hyperfine levels of ^{87}Rb.

N-scheme [14], we observed the fast-light regime without a cavity and also demonstrated that lasing is possible in this scheme.

There are several other proposals for achieving lasing in the fast-light regime. For example, a proposal from the Shahriar group [15] suggests that the presence of two Raman gain lines in the vicinity of each other will provide an absorption-like feature between the gain lines while retaining the positive gain necessary for lasing. For another design from this group, in which an absorptive dip is placed on top of a single Raman gain line [16], indirect measurements suggest an achievable cavity-response enhancement by a factor of 190.

A schematic representation of our experimental setup is shown in Fig. 2. The gyroscope is a square-shaped cavity with perimeter $p = 80$ cm, into which we inject two pump-laser fields tuned to the ^{87}Rb D_1 line (795 nm) and D_2 line (780 nm), respectively. These pumps are first combined using a fiber-optic beam splitter and injected into a solid-state amplifier to boost their total power level to about 200 mW before injecting them into the cavity. The power ratio of the pumps was approximately 1 for all of the data presented here. A cylindrical cell (length 22 mm, diameter 25 mm) filled with isotopically enriched ^{87}Rb vapor and 5 torr of Ne buffer gas is placed

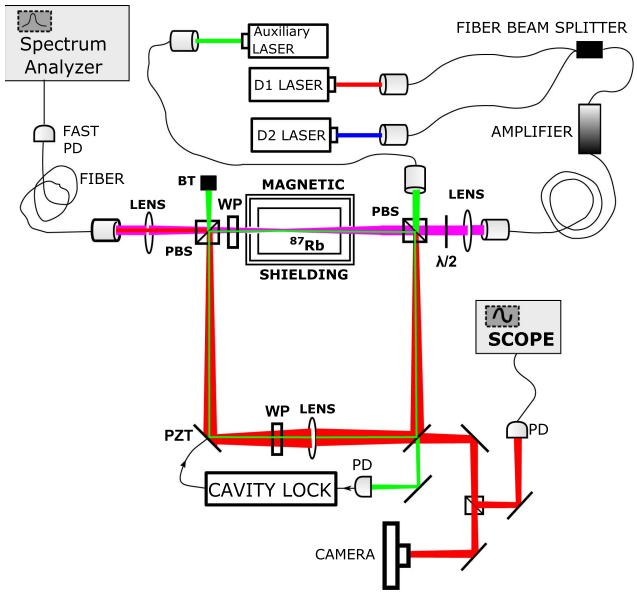

Fig. 2. Schematic of the setup.

inside of a three-layer magnetic shielding and mounted inside the cavity. Two highly reflective flat mirrors and two polarizing beam splitter (PBS) cubes comprise the cavity, as depicted in Fig. 2. To stabilize the cavity, we use an intracavity lens with a focal length of 30 cm. Such a configuration effectively directs the most focused part of the cavity mode inside of the Rb cell. The overall finesse of the empty cavity was about 30–40, largely determined by absorption by the Rb-cell windows (≈0.05–0.10) and intentional polarization distortion by two waveplates (WP), as discussed below.

To control the cavity length, we lock it to an auxiliary narrow-band laser (linewidth ≤100 kHz) that is far detuned from any atomic transitions and thus "sees" the empty cavity, unaffected by the atomic dispersion. The light from this laser is counterpropagating to the pumps' direction to avoid saturation of the output detectors. While most of the auxiliary field passes through a PBS and hits the beam trap (BT), a small polarization rotation, introduced by a WP, transfers a fraction of the auxiliary field into a cavity mode. When locked, the cavity length follows the frequency change of the auxiliary laser (Δf_{empty}).

The pump light's polarization is set so that it can pass through the beam splitters, so the pump fields do not circulate in the cavity. However, the fields α and β are produced with polarization orthogonal to that of the pump, and thus are reflected by the PBSs and can lase when cavity resonant conditions are met. In our setup, the gain line is narrower than the cavity free spectral range, so we have to tune the cavity frequency to match the atomic gain line. Once the cavity detuning is such that it is lasing, we can measure the lasing frequency. This is done by observing the beat note between the D_1 pump and the lasing field on a fast photodiode. The photodiode mostly sees the pump fields passing through the output-cavity PBS. Normally, the lasing field would be fully reflected by this PBS back into the cavity. To allow a small pick-off, we rotate the light polarization by a few degrees using a WP between the atomic cell and the output PBS, so that a small fraction of the lasing field escapes the cavity in the same polarization as the pumps. We can thus observe the beat note between the newly generated field and the corresponding pump occurring at a frequency near the ^{87}Rb ground level splitting (6.8 GHz). The linewidth of each of the beat notes is limited by the spectral-analyzer resolution bandwidth, which was typically set to 300 kHz. Because of the symmetry of the double-Λ system, both α and β fields could be generated, depending on the experimental conditions. While this particular detection scheme does not allow us to discriminate between the beat note of the lasing field α and the D_1 field or the β field and the D_2 field, additional measurements of the generated field frequency confirmed that it was the α field for all the reported data.

To measure the response of the generated-field frequency to cavity-length variations we continuously tune the frequency of the auxiliary laser (to which the cavity is locked), thus changing the empty-cavity detuning (Δf_{empty}), and track the changes in the beat-note-frequency position. Since the pump frequency is held constant, the measured shift corresponds to the lasing-frequency shift ($\Delta f_{\text{dispersive}}$). An example of this can be seen in Fig. 3. Most of the time, the dependence of the lasing detuning on the change in cavity length (and thus on Δf_{empty}) is linear. We define the pulling factor (PF) as the slope of this linear dependence. Combining this definition with Eq. (1), we obtain

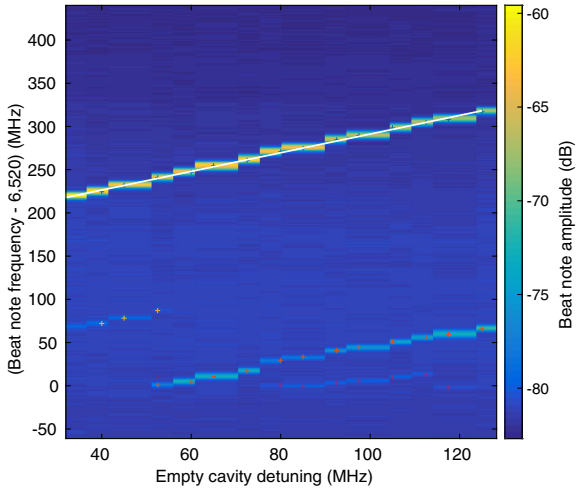

Fig. 3. Beat-note-spectrum dependence on the empty-cavity detuning (cavity length change). The line demonstrates the linear fit used for the pulling factor extraction. Tracks of several competing spatial lasing modes are shown. Note that the tracks have different slopes (pulling factors). The D_2 pump was detuned 120 MHz toward lower frequencies from the $F_g = 2 \rightarrow F_e = 3$ transition. The D_1 pump was detuned 1.5 GHz toward higher frequencies from the $F_g = 1 \rightarrow F_e = 1$ transition. The combined D_1 and D_2 pump power was 230 mW.

$$\mathrm{PF} \equiv \frac{\Delta f_{\mathrm{dispersive}}}{\Delta f_{\mathrm{empty}}} = \frac{1}{n_g}. \tag{2}$$

If PF>1, the laser is in the fast-light regime with enhanced response to changes in the cavity path length. Conversely, for PF<1 the laser is less sensitive to fluctuations in cavity length.

Often we see more than one beat note corresponding to different spatial cavity-lasing modes, as observed by the camera. The different spatial lasing modes have different PFs (seen as separate lines with different slopes in Fig. 3). For the results presented below, we show only the mode that exhibited the greatest cavity response. Typically, this mode was the TEM_{00} spatial lasing mode, which was usually the strongest.

Figure 4 presents measurements of the PF as we varied the D_2 pump detuning from the Rb $F_g = 2 \rightarrow F_e = 3$ transition, keeping the D_1 pump laser frequency fixed at +1.5 GHz above the $F_g = 1 \rightarrow F_e = 1$ transition. We did measurements in two different regimes. In the "low-pump-power, low-atomic-density" regime, we set the total pump power at 6 mW and maintained the Rb cell temperature at 80°C (corresponding to the atomic density $n = 1.5 \times 10^{12}$ cm^{-3}). In the "high-pump-power, high-atomic-density" regime, we increased the total pump power to either 208 mW or 178 mW and were able then to operate at a higher Rb cell temperature of 100°C (atomic density $n = 6.0 \times 10^{12}$ cm^{-3}).

We see that in the high-pump-power regime there is a slight trend toward higher PF as we increase the D_2 pump frequency. The PF reaches nearly unity as we approach approximately 200 MHz, at which point the lasing stops. On the other hand, the low-pump-power regime exhibits a dispersion-like dependence of the PF on the D_2 laser detuning. It reaches maximum when the D_2 detuning matches the $F_g = 2 \rightarrow F_e = 3$ transition and drops to almost zero as we increase the detuning further. We note that the low-pump-power regime is associated

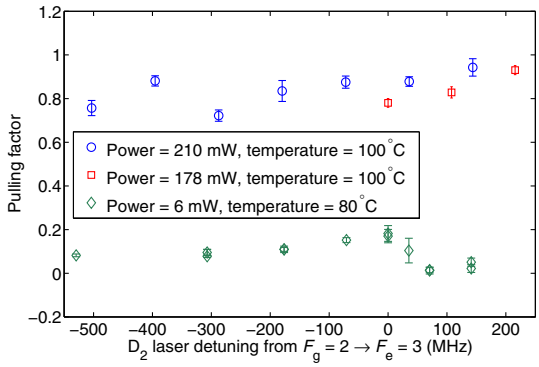

Fig. 4. PF versus D_2 detuning data from the $F_g = 2 \rightarrow F_e = 3$ transition. The blue circle markers indicate data collected at a total power of 210 mW, red squares at a total power of 178 mW, and green diamonds at a total power of 6 mW. Both the blue circle data and the red square data were collected at a fixed Rb cell temperature of 100°C. Likewise, the green diamond markers indicate data collected at a temperature of 80°C. All measurements were taken at a fixed D_1 detuning of 1.5 GHz towards higher frequencies from the $F_g = 1 \rightarrow F_e = 1$ transition. The error bars represent the uncertainty of the linear fit used for the PF extraction.

with much weaker lasing power, which is expected, since the output power is related to the pumping strength.

The drastic difference in PF for high- and low-power regimes can be explained as follows. In general, the lasing frequency is dictated by the convolution of the cavity mode line and the amplification spectrum of the FWM atomic process. Since at low pump powers the atomic gain line is substantially narrower than the cavity linewidth, the lasing frequency is mainly governed by the FWM resonant frequency, as long as it falls within the allowed cavity mode, as discussed in our previous work [14]. In the high-power regime, the power-broadened atomic gain line is wider than the cavity line, so the lasing frequency mostly follows the cavity detuning.

Next, we studied the dependence of the PF on atomic density. The results are shown in Fig. 5. It is expected that with

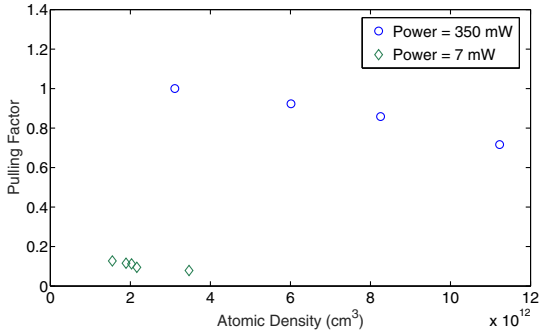

Fig. 5. PF versus atomic density. Both sets of measurements were taken at a fixed D_1 pump detuning of 1.5 GHz towards higher frequencies from the $F_g = 1 \rightarrow F_e = 1$ transition. The blue circle data were collected with a D_2 pump detuning of 110 MHz towards lower frequencies from the $F_g = 2 \rightarrow F_e = 3$. The green diamond data were observed for a D_2 pump detuning of approximately 170 MHz towards lower frequencies from the $F_g = 2 \rightarrow F_e = 3$ transition. For the blue circle data, the total pump power was maintained at approximately 350 mW, while the green diamond data were collected at approximately 7 mW.

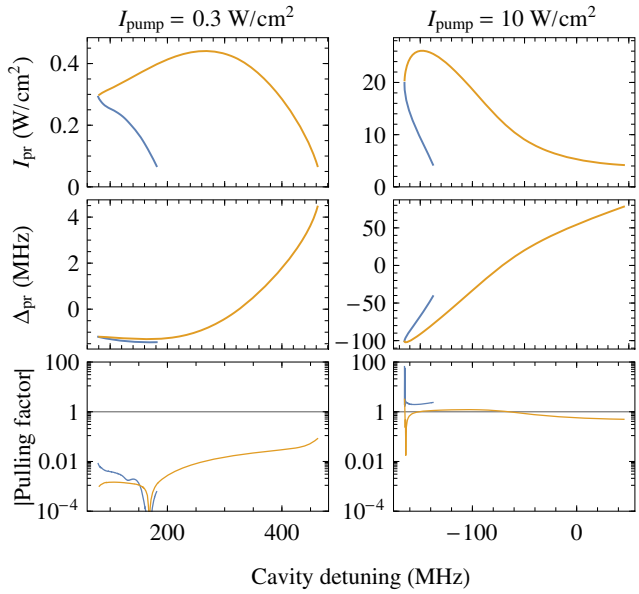

Fig. 6. Numerical simulation results for intracavity probe power (top row), generated probe detuning (middle row), and absolute value of the pulling factor (bottom row) for the "low" (300 mW/cm^2) pump intensity (left column) and for the "high" (10^4 mW/cm^2) pump intensity (right column). Different colors represent different solutions for which lasing is possible under the given conditions.

increased atomic density, the dispersive-cavity properties will increasingly differ from those of an empty cavity, and the PF will deviate from unity. This behavior is very clear in Fig. 5: in the high-density and high-pump-power regime, the PF changes from 1 to approximately 0.7. In the low-power regime, the PF is small even in the low-density regime, but we also see a decrease of the PF with the increase of atomic density.

To better understand the prospects for extending the laser operation into the superluminal regime, we also conducted numerical simulations of probe-field generation for the four-level system shown in Fig. 1, including the effects of Doppler broadening. For a given set of pump parameters, the cavity round-trip complex amplitude gain for the probe light is calculated as a function of probe-field intensity and detuning, using the method described in Ref. [14]. For lasing to occur, we require unity round-trip gain; the probe intensities and detunings at which this happens are found as a function of cavity tuning. Figure 6 shows results of the calculation with the D_1 pump tuned 1.5 GHz above the optical resonance and the D_2 pump on resonance. The round-trip empty-cavity amplitude gain is set to 0.9 (corresponding to a finesse of 30), and the atomic density is 1.2×10^{12} cm^{-3} (lower than the experimental value to offset differences between the four-level system and the full hyperfine structure of Rb). Probe intensity I_{pr}, detuning Δ_{pr}, and absolute value of the pulling factor (derivative of probe detuning with respect to cavity tuning) are shown for two pump intensities, roughly matching the experimental low- and high-pump-intensity regimes. Since there may be more than one combination of I_{pr} and Δ_{pr} at which lasing can occur for each cavity tuning, different branches are represented by differently colored lines.

One can see that the calculated behavior qualitatively matches the experimental observations. For all stable modes, the PFs are smaller than one for the most part, approaching unity at high pump intensity. However, even at lower pump intensity, there are certain places where the probe detuning versus cavity tuning plot has very steep slope, resulting in a PF much greater than one over a narrow cavity tuning range. Observing this regime experimentally will require more precise mode control than allowed by our current approach for measuring the PF, and thus it is not surprising that we were not able to demonstrate this high PF experimentally.

In conclusion, we have shown that through a suitable choice of parameters, one can change the laser PF by more than an order of magnitude. While we were not able to demonstrate the fast-light regime in our lasing system, we showed that we can bring the laser to the regime where its sensitivity to cavity-length perturbations is reduced to 0.014 ± 0.012 of its classical counterpart. Such a reduced sensitivity regime is of interest for the stable laser frequency systems used in metrology.

Funding. Naval Air Warfare Center, Aircraft Division (NAWCAD) (N68335-13-C-0227).

Acknowledgment. We would like to thank Matt Simons and ShuangLi Du for help with initial setup construction.

REFERENCES

1. A. Siegman, *Lasers* (University Science Books, 1986).
2. B. P. Abbott, et al., Phys. Rev. Lett. **116**, 061102 (2016).
3. C. J. Hood, M. S. Chapman, T. W. Lynn, and H. J. Kimble, Phys. Rev. Lett. **80**, 4157 (1998).
4. G. E. Stedman, Rep. Prog. Phys. **60**, 615 (1997).
5. A. A. Velikoseltsev, D. P. Luk'yanov, V. I. Vinogradov, and K. U. Shreiber, Quantum Electron. **44**, 1151 (2014).
6. M. S. Shahriar, G. S. Pati, R. Tripathi, V. Gopal, M. Messall, and K. Salit, Phys. Rev. A **75**, 053807 (2007).
7. M. Sabooni, Q. Li, L. Rippe, R. K. Mohan, and S. Kröll, Phys. Rev. Lett. **111**, 183602 (2013).
8. D. D. Smith, H. Chang, L. Arissian, and J. C. Diels, Phys. Rev. A **78**, 053824 (2008).
9. K. Myneni, D. D. Smith, J. A. Odutola, and C. A. Schambeau, Phys. Rev. A **85**, 063813 (2012).
10. D. D. Smith, K. Myneni, J. A. Odutola, and J. C. Diels, Phys. Rev. A **80**, 011809 (2009).
11. M. S. Shahriar, R. Tripathi, G. S. Pati, V. Gopal, K. Salit, and M. Messall, *Frontiers in Optics* (Optical Society of America, 2005), paper FTuCC3.
12. D. D. Smith, H. A. Luckay, H. Chang, and K. Myneni, Phys. Rev. A **94**, 023828 (2016).
13. N. B. Phillips, I. Novikova, E. E. Mikhailov, D. Budker, and S. Rochester, J. Mod. Opt. **60**, 64 (2013).
14. E. E. Mikhailov, J. Evans, D. Budker, S. M. Rochester, and I. Novikova, Opt. Eng. **53**, 102709 (2014).
15. G. S. Pati, M. Salit, K. Salit, and M. S. Shahriar, Phys. Rev. Lett. **99**, 133601 (2007).
16. J. Yablon, Z. Zhou, M. Zhou, Y. Wang, S. Tseng, and M. S. Shahriar, Opt. Express **24**, 27444 (2016).